An Optimal Regulation of Fluxes Dictates Microbial Growth In and Out of Steady-State

Griffin Chure and Jonas Cremer

Department of Biology, Stanford University, Stanford, CA, USA.

gchure@stanford.edu, jbcremer@stanford.edu

January 27, 2022

Abstract

Effective coordination of cellular processes is critical to ensure the competitive growth of microbial organisms. Pivotal to this coordination is the appropriate partitioning of cellular resources between protein synthesis via translation and the metabolism needed to sustain it. Here, we present a coarse-grained and organism-agnostic theory of microbial growth centered on the dynamic regulation of this resource partitioning. At the core of this regulation is an optimization of metabolic and translational fluxes, mechanistically achieved via the perception of charged- and uncharged-tRNA turnover. An extensive comparison with ≈ 50 data sets from *Escherichia coli* establishes the theory's veracity and shows that it can predict a remarkably wide range of growth phenomena in and out of steady-state with quantitative accuracy. This predictive power, achieved with only a few biological parameters, cements the preeminent importance of protein synthesis in microbial growth and establishes the theory as an ideal physiological framework to interrogate the dynamics of growth, competition, and adaptation in complex and ever-changing environments.

Introduction

Growth and reproduction is central to life. This is particularly true of microbial organisms where the ability to quickly accumulate biomass is critical for competition in ecologically diverse habitats. Understanding which cellular processes are key in defining growth has thus become a fundamental goal in the field of microbiology. Pioneering physiological and metabolic studies throughout the 20th century laid the groundwork needed to answer this question [1–11], with the extensive characterization of cellular composition across growth conditions at both the elemental [12–14] and molecular [7, 8, 15, 16] levels showing that the dry mass of microbial cells is primarily composed of proteins and RNA. Seminal studies further revealed that the cellular RNA content is strongly correlated with the growth rate [7, 8, 17], an observation which has held for many microbial species [18]. As the majority of RNA is ribosomal, these observations suggested that protein synthesis via ribosomes is a major determinant of biomass accumulation in nutrient replete conditions [19–21]. Given that the cellular processes involved in biosynthesis, particularly those of protein synthesis, are well conserved between species and domains [22–24], these findings have inspired hope that fundamental principles of microbial growth can be found despite the enormous diversity of microbial species and the variety of habitats they occupy.

The past decade has seen a flurry of experimental studies further establishing the importance of protein synthesis in defining growth. Approaches include modern "-omics" techniques with molecular-level resolution [25–38], measurements of many core physiological processes and their coordination [39–44], and the perturbation of major cellular processes like translation [39, 45–47]. Together, these studies have provided a new level of description quantifying how cells allocate their ribosomes to the synthesis of different proteins depending on their metabolic state and the environmental conditions they encounter, a process we here call *ribosomal allocation*. Tied to the experimental studies, low-dimensional models [48, 49] have been formulated to dissect how ribosomal allocation influences growth. These *ribosomal allocation models*, which incorporate only a few parameters, can help to

rationalize growth and proteomic composition in both static and dynamic environments [31, 47, 50–55] (a more detailed overview is provided in Supplementary Text 1). However, these models are largely phenomenological, bespoke to specific data sets, and require redefinition of the mathematics from scenario to scenario, significantly hampering their predictive power.

In this work, we overcome these limitations by establishing and systematically probing a self-consistent theory of ribosomal allocation capable of predicting the dynamics of growth in and out of steady-state and across physiological perturbations. At the core of the model is the dynamic regulation of allocation which changes with the metabolic state of the cell. We demonstrate how an optimal allocation promoting rapid growth emerges when the flux of translation to generate new proteins and the flux through metabolism to provide new precursors are mutually maximized given the environmental conditions and the corresponding physiological constraints. This regulation scheme, which we term *flux-parity regulation*, can be mechanistically achieved by a global regulator (such as guanosine tetraphosphate, ppGpp, in bacteria) capable of simultaneously measuring the turnover of charged- and uncharged-tRNA pools. To probe the explanatory of our approach and the fundamental behavior of flux-parity regulation, we compare model predictions with ≈ 50 data sets from *Escherichia coli*, spanning more than half a century of studies. The theory describes a broad and diverse range of phenomena – including the fundamental relationships seen in steady-state, the response to fluctuating environments, and the consequences of physiological stresses. The accuracy of the predictions coupled with the minimalism of the model cements the centrality of protein synthesis in defining microbial growth. Furthermore, the mechanistic nature of the theory – predicated on a minimal set of biologically meaningful parameters – provides a framework that can be used to explore complex phenomena at the intersection of physiology, ecology, and evolution.

Results

The Cell as a Proteinaceous Self-Replicator

We here consider a well-mixed environment containing a clonal population of growing microbial cells [diagrammed in Figure 1(A)]. That is, we treat all cells as being identical and encountering the same conditions, including the nutrients which they consume to build new cellular material. As the dry mass of microbial cells is primarily protein [56, 57], and proteins are costly to make [33, 58], we focus on protein synthesis as the central biochemical process defining growth. Rather than considering the abundance of thousands of unique protein species within a cell, we take a coarse-grained view of the composition of the proteome (similar to previous modeling approaches [45,48,49]) where proteins are pooled together and assigned to be either ribosomal (i.e. synthesizing new protein from precursors such as charged-tRNA), metabolic (i.e. synthesizing precursors from nutrients), or being involved in other biological processes required for cellular growth and survival [Fig. 1(A)]. To keep the dynamics simple, we furthermore do not consider individual cells in the culture (which would require careful consideration of cell sizes and the intricate coupling between size and growth) but rather describe how the total (protein) biomass increases over of time.

This low-dimensional view of the cell and biological matter may at first seem like an unfair approximation, ignoring the decades of work interrogating the myriad biochemical and biophysical processes of cell-homeostasis and growth [46, 59–62]. However, at least in nutrient replete conditions, many of these processes appear not to impose a fundamental limit on the rate of growth in the manner that protein synthesis does (Supplementary Text 2); the vast majority of processes are "parallelizeable" and their regulation is such that they do not become rate-limiting. For *E. coli* this was systematically considered for an array of processes [33]. For example, the copy numbers of rRNA genes cells carry on their chromosome are sufficiently high to prevent rRNA synthesis becoming a bottleneck of growth. Furthermore, *E. coli* can copy its chromosome in parallel along several replication forks allowing a division time shorter than the replication time of a single chromosome. Protein synthesis, in contrast, imposes a strict bottleneck on the speed of growth. This can be illustrated with a flux diagram [Fig. 1(C), [31, 33, 49, 51]] describing the masses of precursors, proteins, and nutrients (gray boxes) and their flux through biochemical processes (white boxes). The diagram emphasizes that growth is autocatalytic in that the synthesis of ribosomes is undertaken by ribosomes. Fast growth thus requires a large number of ribosomes making new ribosomes. However, more proteins than ribosomes are needed for growth to proceed, particularly metabolic proteins which provide the precursors required for ribosomes to work. This aspect is the crux of the ribosomal allocation model: the abundance of ribosomes is constrained by

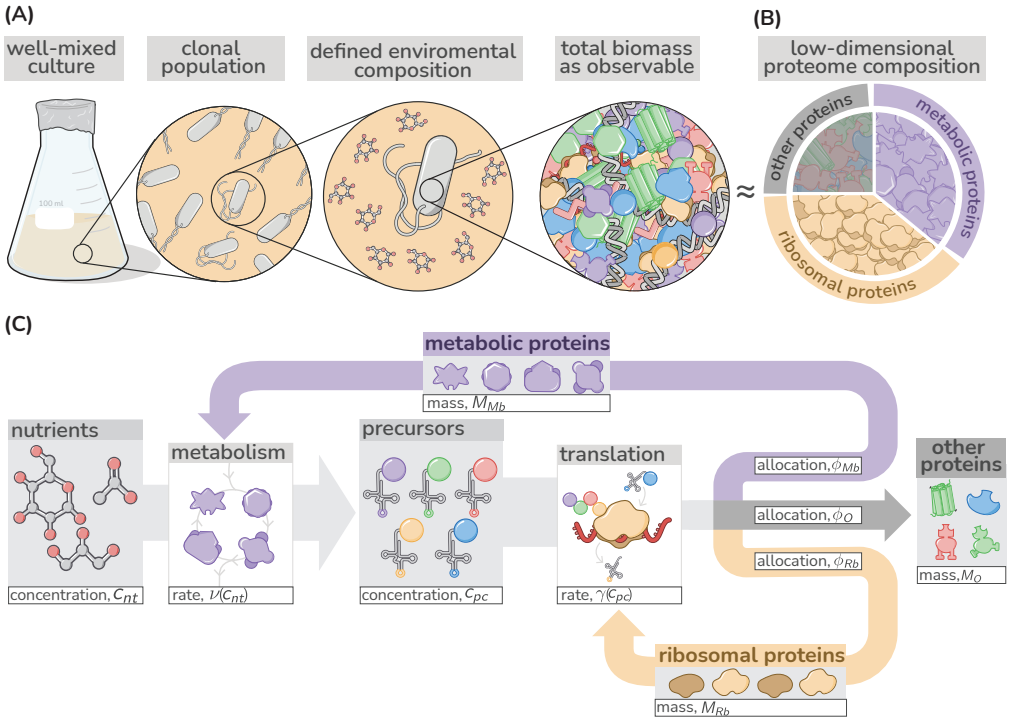

Figure 1: Growth and mass flow through a proteinaceous self-replicating system.(A) The model considers growth of a clonal population in a well-defined mixed environment. Key observables are the protein biomass in the system and its accumulation. (B) The total proteomic composition is coarse-grained into being composed of metabolic proteins (purple), ribosomal proteins (gold), or "other" proteins (gray). (C)The flow of mass through the self-replicating system. Biomolecules and biosynthetic processes are shown as grey and white boxes, respectively. Nutrients in the environment passed through cellular metabolism to produce "precursor" molecules, here diagrammed as charged-tRNA molecules. These precursors are consumed through the process of translation to produce new protein biomass, either as metabolic proteins (purple arrow), ribosomal proteins (gold arrow), or "other" proteins (gray arrow). The mathematical symbols as used in the ribosomal allocation model are indicated.

the need to synthesize other proteins and growth is a result of how new protein synthesis is partitioned between ribosomal, metabolic, and other proteins. How is this partitioning determined, and how does it affect the dynamics of growth? To answer these questions, we must understand how this biological system functions at a quantitative level and we thus seek to mathematize the biology underlying the boxes and arrows in Fig. 1(C), beginning with the dynamics of protein synthesis.

Synthesis of Proteins

The rate of protein synthesis is determined by two quantities – the total number of ribosomes N_{Rb} and the speed v_{tl} at which they are translating. The latter depends on the concentration of precursors needed for peptide bond formation, such as tRNAs, free amino acids, and energy sources like ATP and GTP. Taking the speed v_{tl} as a function of the concentration of the collective precursor pool c_{pc}, the increase in protein biomass M follows as

$$\frac{dM}{dt} = v_{tl}(c_{pc})N_{Rb}. \tag{1}$$

There exists a maximal speed at which ribosomes can operate, v_{tl}^{max}, that is reached under optimal conditions when precursors are highly abundant, in *E. coli* approximately 20 amino acids (AA) / second (s) [63]. Conversely, the translation speed falls when precursor concentrations c_{pc} get sufficiently small. Simple biochemical considerations support a Michaelis-Menten relation [33, 64, 65] as good approximation of this behavior with the specific form

$$v_{tl}(c_{pc}) = v_{tl}^{max}\left(\frac{c_{pc}}{c_{pc} + K_M^{c_{pc}}}\right), \tag{2}$$

where $K_M^{c_{pc}}$ is a Michaelis-Menten constant with the maximum speed v_{tl}^{max} only observed for $c_{pc} \gg K_M^{c_{pc}}$. The number of ribosomes N_{Rb} can be approximated given knowledge of the total mass of ribosomal proteins M_{Rb} and the proteinaceous mass of a single ribosome m_{Rb} via $N_{Rb} \approx M_{Rb}/m_{Rb}$(more details in Supplementary Text 3). The increase in protein biomass (Eq. 1) is thus

$$\frac{dM}{dt} = v_{tl}(c_{pc})\frac{M_{Rb}}{m_{Rb}} \equiv \gamma(c_{pc})M_{Rb}. \tag{3}$$

The *translation rate* $\gamma(c_{pc}) \equiv v_{tl}(c_{pc})/m_{Rb}$ describes the rate at which ribosomes generate new protein.

The maximal translation rate $\gamma_{max} \equiv v_{tl}^{max}/m_{Rb}$ imposes a firm upper limit of how rapidly biomass can accumulate, unrealistically assuming the system would consist of only ribosomes translating at maximum rate. Notably, however, this upper limit is not much faster than the fastest growth observed, highlighting the importance of protein synthesis in defining the timescale of growth. For example, the maximal translation rate for *E. coli* is ≈ 10 hr^{-1} and thus only ≈ 4 times higher than the growth rates in rich LB media ($\lambda \approx 2.5$ hr^{-1}). Including the synthesis of rRNA, another major component of the cellular dry mass, lowers this theoretical limit only marginally, further supporting our sole consideration of protein synthesis in defining growth (Supplementary Text 4). The difference between measured growth rates and the theoretical limits can be mostly attributed to the synthesis of metabolic proteins which generate the precursors required for protein synthesis, which we consider next.

Synthesis of Precursors

Microbial cells are generally capable of synthesizing precursors from nutrients available in the environment, such as sugars or organic acids. This synthesis is undertaken by a diverse array of metabolic proteins ranging from those which transport nutrients across the cell membrane, to the enzymes involved in energy generation (such as those of fermentation or respiration), and the enzymes providing the building blocks for protein synthesis (such as those involved in the synthesis of amino acids). While these enzymes vary in their abundance and kinetics, we group them all into single set of metabolic proteins with a mass M_{Mb} which cooperate to synthesize the collective pool of precursors from nutrients required for protein synthesis. We make the approximation that these metabolic proteins generate precursors at an effective *metabolic rate* ν, which depends on the concentration of nutrients c_{nt} in the environment. Canonically, such a relation is described by a Monod (Michaelis-Menten) relation

$$\nu(c_{nt}) = \nu^{max}\left(\frac{c_{nt}}{c_{nt} + K_M^{c_{nt}}}\right), \tag{4}$$

where ν_{max} is the maximum metabolic rate describing how fast the metabolic proteins can convert nutrients to precursors, and $K_M^{c_{nt}}$ is the Monod constant describing the concentration below which nutrient utilization slows [66]. Novel precursors are thus supplied with a total rate of $\nu(c_{nt})M_{Mb}$ and consumed via protein synthesis at a rate $\gamma(c_{pc})M_{Rb}$. Translation relies on precursors and, as introduced above, the translation rate $\gamma(c_{pc})M_{Rb}$ thus depends on the concentration of precursors in the cell, c_{pc}. As we do not explicitly model cell division, we here approximate this cellular concentration as the relative mass abundance of precursors to total protein biomass. This approximation is justified by the observation that cellular mass density and total protein content is approximately constant across a wide range of conditions [33, 67, 68] (Supplementary Text 2). The dynamics of precursor concentration follows from the balance of synthesis, consumption, and dilution as the total biomass grows:

$$\frac{dc_{pc}}{dt} = \overbrace{\frac{\nu(c_{nt})M_{Mb}}{M}}^{\text{production via metabolism}} - \underbrace{\frac{\gamma(c_{pc})M_{Rb}}{M}}_{\text{consumption via protein synthesis}} - \overbrace{\frac{c_{pc}\gamma(c_{pc})M_{Rb}}{M}}^{\text{dilution via growth}}. \tag{5}$$

While the dilution term is commonly assumed to be negligible, this term is critical to describe growth and derive analytical expressions (detailed discussion in Supplementary Text 5).

Consumption of Nutrients

The synthesis of novel precursors relies on the availability of nutrients which changes depending on the environment. Here we consider specifically a "batch culture" scenario [Fig.1(A)] in which nutrients are provided only at the beginning of growth and are never replenished. Therefore, growth of the culture continues until all of the nutrients have been consumed. The concentration of nutrients in the environment is thus given as

$$\frac{dc_{nt}}{dt} = -\frac{\nu(c_{nt})M_{Mb}}{Y}, \tag{6}$$

where Y is the yield coefficient which describes how many nutrient molecules are needed to produce one unit of precursors.

Ribosomal Allocation of Protein Synthesis

As final step of the model definition, we must describe how cells direct their protein synthesis towards making ribosomes, metabolic proteins, or all other proteins that make up the cell [colored arrows in Fig. 1(A)]. We do so by introducing three *allocation parameters* ϕ_{Rb}, ϕ_{Mb}, and ϕ_O (such that $\phi_{Rb} + \phi_{Mb} + \phi_O = 1$) which define how novel protein synthesis is partitioned among these categories:

$$\frac{dM_{Rb}}{dt} = \phi_{Rb}\frac{dM}{dt}\ ;\ \frac{dM_{Mb}}{dt} = \phi_{Mb}\frac{dM}{dt}\ ;\ \frac{dM_O}{dt} = \phi_O\frac{dM}{dt}. \tag{7}$$

Growth Dynamics and the Emergence of a Steady-State Regime

These equations are summarized in Fig. 2 and define the accumulation of biomass, from nutrient uptake to protein synthesis. The coarse grained model is described by a handful parameters with distinct biological meaning and that can be directly measured or estimated as we discuss further below. Using a parameter set descriptive of the model organism *E. coli*, we first explore the dynamics that emerge. As experimentally observed, initially abundant nutrients are consumed and biomass accumulates (exponential phase) until nutrients are exhausted and growth stops (saturation phase) [Figure 2 (B) and (C)]. Importantly, precursor concentrations [Fig. 2(C)] quickly reach a constant plateau which lasts until nutrients become scare ($c_{nt} \gg K_M^{c_{nt}}$ and $\nu(c_{nt}) \approx \nu_{max}$). During this transient period [shaded regions in Fig. 2(B-D)], and the synthesis of precursors matches the consumption by protein synthesis and dilution, meaning

$$\frac{dc_{pc}}{dt} = 0. \tag{8}$$

Given a constant precursor concentration c^*_{pc}, the translation rate $\gamma(c^*_{pc})$ is also constant. As a consequence, the protein pool approaches a steady composition dictated by the allocation parameters such that

$$\frac{M_{Rb}}{M} = \phi_{Rb}\ ;\ \frac{M_{Mb}}{M} = \phi_{Mb}\ ;\ \frac{M_O}{M} = \phi_O. \tag{9}$$

With precursor concentrations and protein composition remaining constant, the system is in a *steady-state* and biomass accumulates exponentially over time,

$$\frac{dM}{dt} = \gamma(c^*_{pc})\phi_{Rb}M \equiv \lambda M. \tag{10}$$

with constant growth-rate $\lambda \equiv \gamma(c^*_{pc})\phi_{Rb}$. To further illustrate how parameters shape growth and the emergence of a steady state, an interactive version of Fig. 2 is hosted on the associated paper website. Notably, as long as we consider the dilution of precursors, the steady state growth regime emerges directly from the introduced dynamics and does not rely on additional mechanisms like an inhibition of metabolism at high precursor concentrations (Supplementary Text 5). Explicitly modeling the dilution of precursors also allows us to derive a suite of analytical expressions for the precursor concentration c^*_{pc}, the translation rate $\gamma(c^*_{pc})$, and the growth rate λ [Fig. 3(A; boxes) and Supplemental Text 6]. With these expressions in hand we now discuss how growth rates vary with ribosomal allocation. Fig. 3(A-C, red lines) shows the steady state solutions when varying the allocation towards ribosomal and metabolic

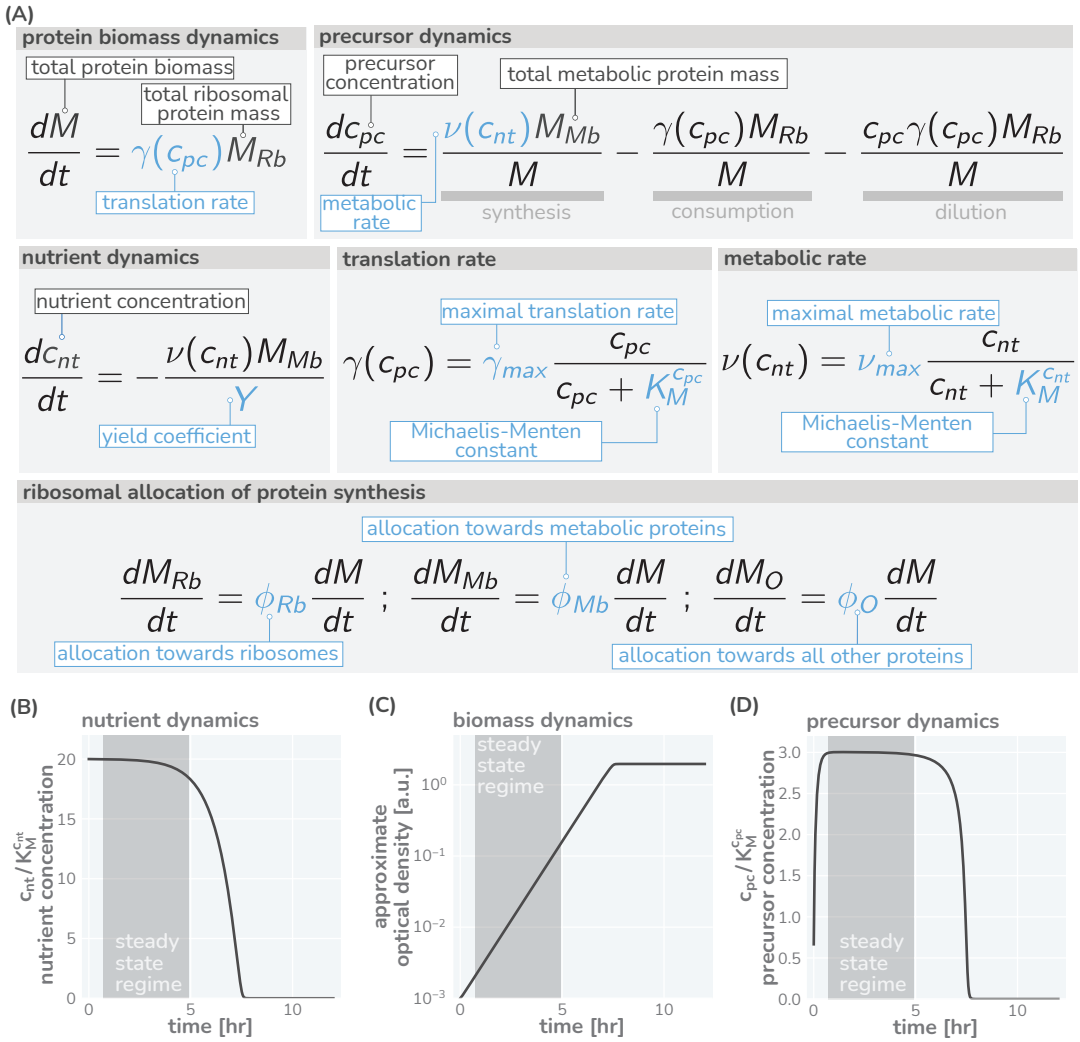

Figure 2: The governing dynamics of the ribosomal allocation model.(A) Annotated equations of the model with parameters highlighted in blue. Integrated temporal dynamics of these equations are shown for (B) the environmental nutrient concentration, (C) biomass accumulation, and (D) the precursor concentration. The parameters chosen for this integration are provided in Supplemental Table 1 and approximate the growth of *E. coli* in a glucose-minimal medium with a growth rate of ≈ 1 / hr. Initial nutrient concentration is taken to be ≈ 10 mM. Biomass units are approximately converted to optical density assuming at $OD_{600nm} = 1$, there are 10^9 cells per mL and 10^9 amino acids per cell. An interactive version of these dynamics can be found on the paper website.

proteins [purple and gold arrows in Fig. 1(B)] while keeping all other parameters fixed using the same reference parameter set as before (an interactive version is hosted on the associated paper website). Importantly, there exists an optimal allocation which optimizes growth: If the allocation towards ribosomal proteins ϕ_{Rb} is too high and the allocation towards metabolic proteins ϕ_{Mb} too low, there will be plenty of ribosomes available to synthesize proteins but not enough precursors do so efficiently; precursor concentrations (panel A) and thus translation rates (panel B) are low, resulting in slow growth (panel C). Conversely, if the allocation towards metabolic proteins ϕ_{Mb} is too high and the allocation towards ribosomal proteins ϕ_{Rb} too low, precursors are supplied in excess (panel A) and translation rates are high (panel B), but the ribosome content is low, limiting protein synthesis and slowing growth (panel C). This trade-off between metabolic and ribosomal protein content can also be seen in Eq. 10. Fast growth relies on a large ribosomal allocation ϕ_{Rb}, but metabolic proteins are also needed to maintain a precursor concentration such that translation $\gamma(c^*_{pc})$ is rapid.

Regulation of allocation

The strong dependence of growth on the ribosomal and metabolic protein content highlights that cells need to fine-tune the regulation of protein synthesis depending on their metabolic state and the environmental conditions they encounter. To explore this regulation, we now consider growth depends on the metabolic rate ν_{max} which describes how fast metabolic proteins transform nutrients into precursors and can thus be seen as a measure of the nutrient quality (with small and large values of ν_{max} corresponding to poor and rich conditions). The different colored lines in Fig. 3(A-C) show the precursor concentration, translation rate, and growth rate for a range of metabolic rates ν_{max}. The allocation which optimizes growth rate (Fig.3C) varies strongly with the metabolic rates [points in Fig. 3(A-C)]. The strong dependence highlights a question critical to understand microbial growth: How do cells tune their allocation of protein synthesis to arrive at a specific growth rate? To approach this question, we here first discuss three regulatory strategies which microbes may employ to coordinate allocation with encountered conditions.

Scenario I: Constant Allocation

We first consider a scenario in which the allocation parameters are fixed and do not vary with conditions (Fig. 3(D-G), black box and lines). Locking in the ribosome allocation to $\phi_{Rb} = 0.25$ [Fig. 3(E), black line], for example, carries strong consequences for translation and growth rates as illustrated in Fig. 3 (F and G, black lines). When conditions are poor (ν_{max} is small), the translation rate is significantly lower than the maximal rate as there are too many ribosomes competing for a small pool of precursors [Fig. 3(F)]. The translation and growth rates increase with the metabolic rate ν_{max} until the influx of precursors is sufficiently high such that all ribosomes are translating close to their maximum and growth-rate is at its optimal value. Further increasing the metabolic rate does not increase the growth rate [plateau of black curve in Fig. 3(G)] as all ribosomes are already translating close to their maximum rate.

Scenario II: Constant Translation Rate

We next consider a regulatory scheme where the allocation is adjusted such that the translation rate is always close to its maximum value [Fig. 3(D-G), green box and lines]. This is achieved by tuning the allocation such that a constant precursor concentration $c^*_{pc} \gg K_M^{c_{pc}}$ is maintained across different metabolic rates ν_{max}: At higher metabolic rates, the metabolic proteins can sustain a higher influx of precursors allowing a larger allocation towards ribosomal proteins ϕ_R [Fig. 3(E and F green line)]. Accordingly, the growth rate continues to increase with higher metabolic rates always exceeding the growth rate of scenario I [Fig. 3(G, green line)].

Scenario III: Optimal Allocation

As a third scenario, we consider that the allocation can be tuned to optimize growth rate across conditions, meaning that the fastest growth rate is achieved given the constrains described by the metabolic rate and other model parameters [Fig. 3(D-G), blue box and lines]. The allocation towards ribosomes ϕ_{Rb} is adjusted with the metabolic rate such that the growth rate rests at the peak of the curves shown in Fig. 3(C). Similarly to scenario II, the allocation towards ribosomes increases with the metabolic rate to couple the protein synthesis to precursor influx [Fig. 3(E, blue line)]. However, in contrast to scenario II, the translation rate is strongly dependent on the metabolic rate [Fig. 3(F, blue line)]. Complete derivations of the analytical expressions stated in Fig. 3(D) are provided in the Supplemental Text 6 and an interactive version of Fig. 3(E-G) is hosted on the associated paper website.

Comparison With Data From *E. coli*

Thus far, our modeling of microbial growth has remained "organism agnostic" without pinning parameters to the specifics of any one microbe's physiology. The scenarios presented in Fig. 3(D-G) thus describe three strategies different organisms may employ to adjust their ribosomal content. To discriminate between these scenarios and probe the coarse-grained model, we now compare model predictions to data from the well characterized bacterium *E.*

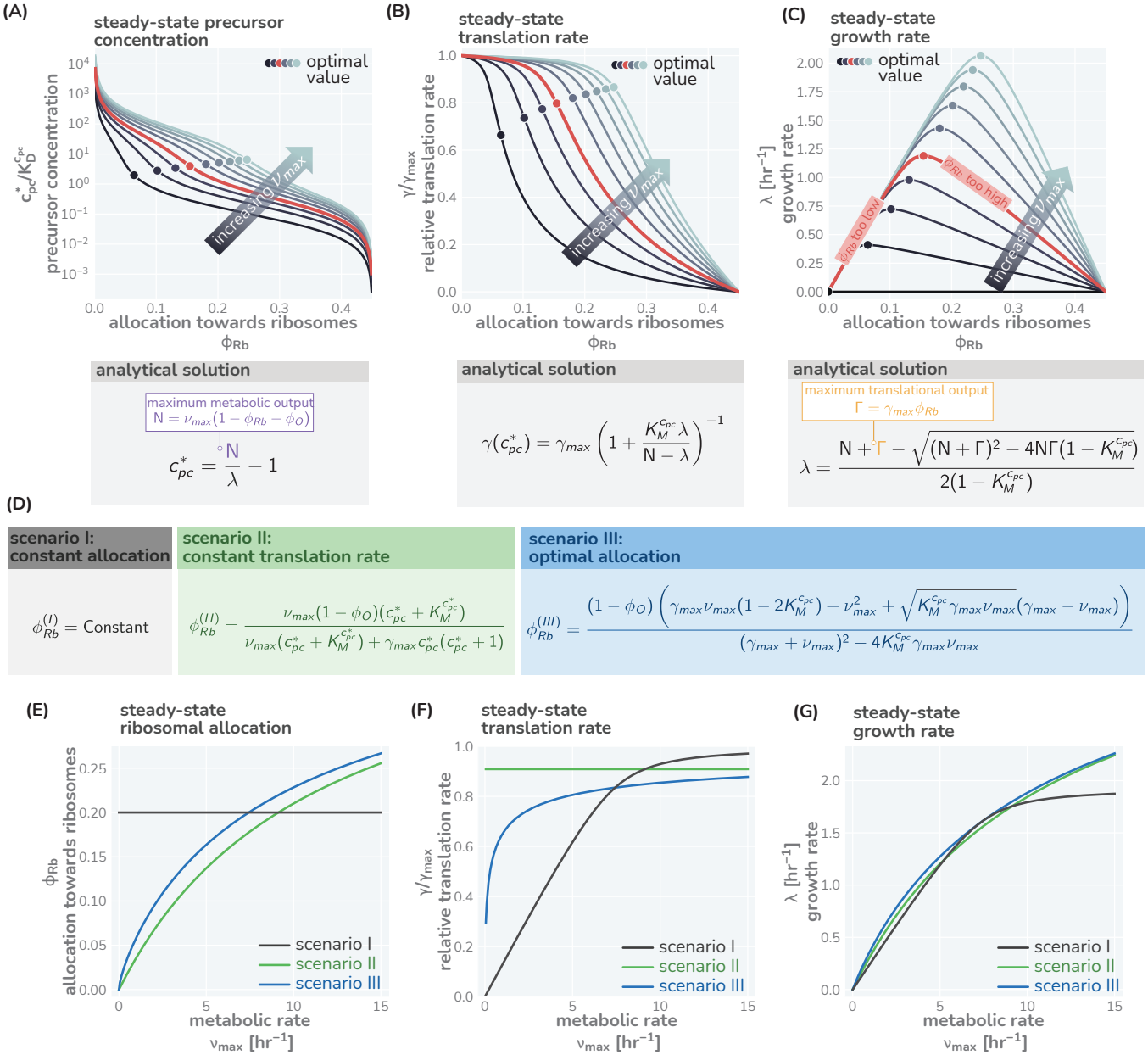

Figure 3: The steady-state dynamics of the ribosomal allocation model and plausible allocation strategies. The steady-state values of (A) the precursor concentration c^*_{pc}, (B) the translation rate $\gamma(c^*_{pc})$, and (C) the growth rate λ are plotted as a function of the ribosomal allocation. The analytical expression for each steady-state quantity is schematized below the respective plot. (D) Analytical solutions for candidate scenarios for regulation of ribosomal allocation with constant allocation, constant translation rate, and optimal allocation highlighted in grey, green, and blue respectively. (E) The behavior of the scenarios for the allocation towards ribosomes, translation rate, and growth rate as a function of ν_{max}. Color coding is the same as in panel (D). Model parameters follow reference set for *E. coli* (Supplementary Table 1) and red lines in (A-C) denotes $\nu_{max} = 4.5$ hr^{-1}, corresponding to growth on glucose. Black lines in (E-G) correspond to a constant allocation $\phi_{Rb}^{(I)} = 0.25$ and green lines correspond to a constant precursor concentration $c^*_{pc} \approx 10K_M^{c_{pc}}$, yielding a constant translation rate of $\gamma(c^*_{pc}) \approx 0.9\gamma_{max}$. An Interactive version of the panels allowing the free adjustment of parameters is available on the associated paper website.

coli. We assembled measurements of ribosome content and translation speeds from 26 different studies spanning 55 years and when cells grew steadily on a wide range of carbon sources covering poor and rich growth conditions (Fig. 4(A) and Supplementary Table 2). These data are shown in Fig. 4(B and C, markers) as a function of the growth rate. To compare the observed trends with model predictions, we then computed ribosome content and translation speed according to the 3 model scenarios when varying the metabolic rate γ_{max} between 0.001 hr^{-1} and 10 hr^{-1} (solid lines) while keeping all other model parameters constant (reference parameter set, Supplementary Table 1).

The strong and well-known [7, 17, 20, 45, 69] correlation between the ribosomal content and the steady-state growth rate [Fig. 4(A)] rules out a condition-independent allocation (black line, scenario I). We can distinguish less confidently between scenario II or III (green and blue lines), however scenario III appears to better describe the data. A clearer distinction is possible when considering the translation speed [Fig. 4(B)]. The observed speed increases non-linearly with the growth rate in strong contrast to scenario II (constant translation rate, green line) but in good agreement with scenario III (optimal allocation, blue line). Deviations from the prediction for scenario III are only evident for the ribosomal content at slow growth ($\lambda \leq 0.5$ hr^{-1}) and can be attributed to additional biological and experimental factors, including protein degradation [70], ribosome inactivation [39, 42], and cultures which have not yet reached steady state (Supplementary Text 7). Overall we thus conclude that scenario III can accurately describe the observations over a very broad range of conditions, supporting the hypothesis that *E. coli* indeed optimally tunes its ribosomal content to promote fast growth. Importantly, the agreement between the theory and observation does not require *ad hoc* fitting of parameters; all fixed model parameters, including the Michaelis-Menten constants and the maximum translation rate, have distinct biological meaning and can be either directly measured or estimated/inferred from data. In Supplemental Table 1, we provide a list of these parameters and values along with the appropriate reference, with consideration of ϕ_O in Supplemental Text 8. Furthermore, there is no combination of parameter values that allow scenario I or II to adequately describe both the ribosomal content and translation speed as a function of growth rate. We discuss the parameter values further in the Supplementary Text 11 and provide an interactive figure (`cremerlab.github.io/flux_parity/data_comparison`) where the parametric sensitivity can be directly explored. We also note that scenario III does not require inclusion of a residual pool of inactive ribosomes to rationalize the offset when describing the change of ribosome content with growth by a linear fit as done in previous phenomenological approaches (Supplementary Text 9).

In Supplemental Text 10, we further present a similar analysis for *S. cerevisiae* which suggests that this eukaryote likely follows an optimal allocation strategy, although data for ribosomal content and translation is scarce. The strong correlation between ribosome content and growth rate has further been reported for other microbial organisms in line with an optimal allocation [18], though the absence of translation speed measurements precludes confirmation. An interesting exception is the methanogenic archaeon *Methanococcus maripaludis* which appears to maintain constant allocation, in agreement with scenario I [71]. The presented analysis thus suggests that *E. coli* and possibly many other microbes closely follow an optimal allocation behavior to support efficient growth. The good agreement between experiments and data establishes that the simple allocation model can describe growth behavior, begging the question: how do cells coordinate their complex machinery to ensure a close to optimal allocation?

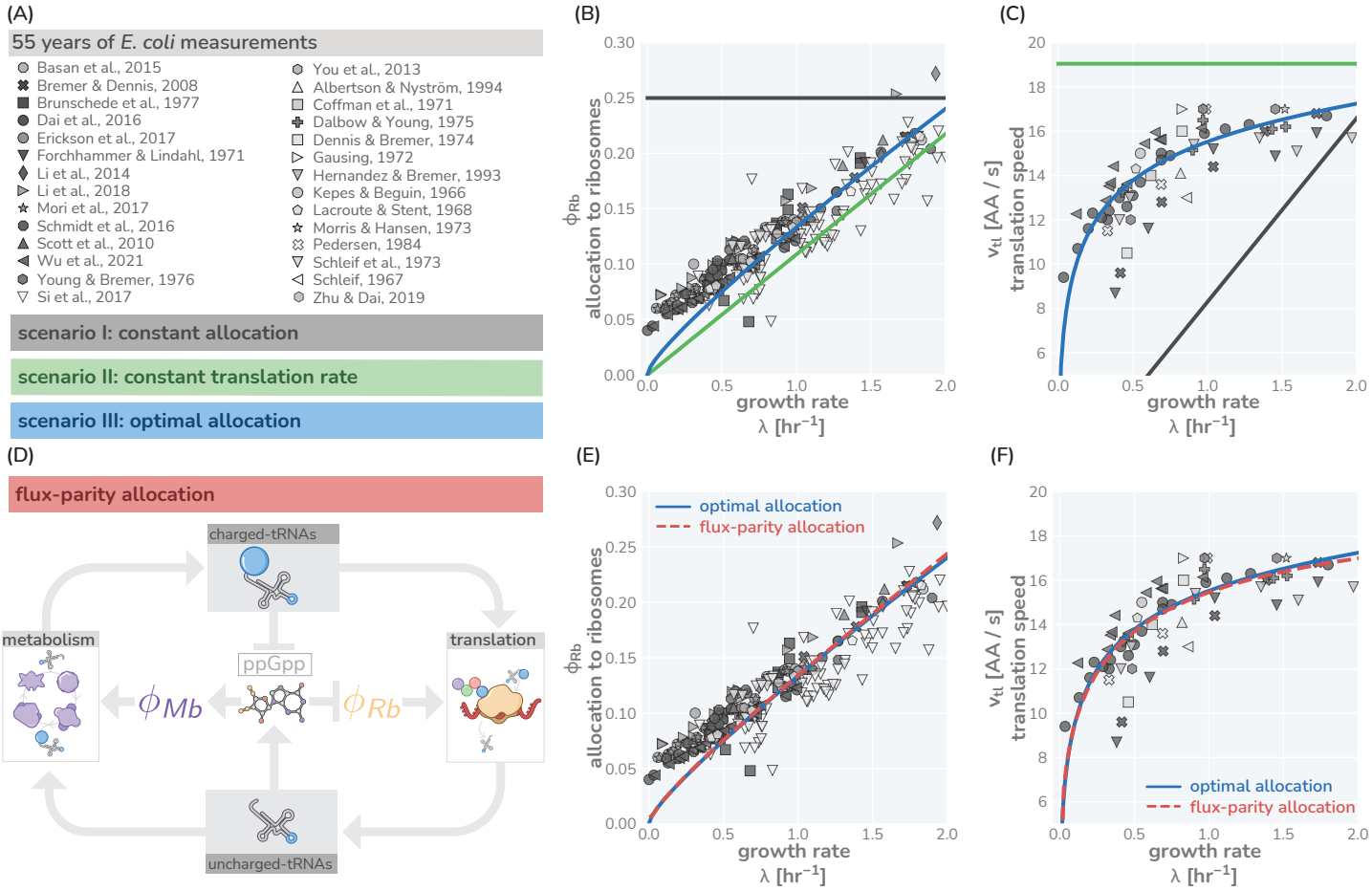

Figure 4: Comparison of model predictions with 55 years of *E. coli* measurements. (A) A list of literature sources reporting measurements for ribosomal content and/or translation speed as a function of the growth rate. More information about these sources are summarized in Supplementary Table 2. (B and C) Comparison of model predictions with literature values for ribosome content and translation speed v_{tl}. Colored lines correspond to predictions from the three scenarios (I: constant allocation, II: constant translation rate, and III: optimal allocation). An interactive version of these panels is hosted on the paper website. (D) A circuit diagram of the regulatory nodes in flux-parity optimization. Metabolic and translational fluxes are connected via a positive feedback loop through the generation of mutual starting materials (uncharged- or charged-tRNAs respectively). The rates of each flux exhibit semi-autoregulatory behavior in that flux through each process reduces the standing pool of tRNAs. Panels (E) and (F) show same data as shown in panel (B) and (C), with the steady-state solution for the flux-parity model shown as a dashed red line. Solid blue line is the solution under scenario III. Solid and dashed lines show model predictions with reference parameter sets, (Supplementary Tables 2 and 3).

Optimal Allocation Results From a Flux-Parity Regulation Mechanism

To optimally tune allocation, cells must have some means of coordinating the expression of metabolic and ribosomal genes such that the rate of protein synthesis is optimized. In the ribosomal allocation model, this reduces to a regulatory mechanism in which the allocation parameters (ϕ_{Rb} and ϕ_{Mb}) are dynamically adjusted such that the metabolic flux to provide new precursors ($\nu\phi_{Mb}$) and translational flux to make new proteins ($\gamma\phi_{Rb}$) are not only equal but are mutually maximized; in this condition, any change of the allocation parameters results in a decrease in the magnitude of either flux. We here term this regulatory scheme *flux-parity regulation* to emphasize the optimization of fluxes in contrast to just the balance of their values (known as flux-balance which is necessarily satisfied in steady-state). Cells can achieve such regulation via a global regulation mechanism which senses the fluxes and controls the expression of genes involved in metabolism and protein synthesis in response. Here, we specifically examine the role of guanosine tetraphosphate (ppGpp), a global regulatory metabolite required by *E. coli* and other prokaryotes to indicate amino acid limitation and to regulate ribosomal and metabolic genes [72–75]. We thus

extend our allocation model and consider allocation parameters which are dependent on the ppGpp concentration,

$$\phi_{Rb} \to \phi_{Rb}([\text{ppGpp}]) \text{ and } \phi_{Mb} = 1 - \phi_O - \phi_{Rb}([\text{ppGpp}]). \tag{11}$$

Mechanistically, ppGpp levels are enzymatically controlled depending on the metabolic state of the cell, for example via the relative availability of charged and uncharged-tRNA. However, many molecular details of this regulation remain unclear [72, 73, 75]. Rather than explicitly mathematizing the biochemical dynamics of ppGpp synthesis and degradation, as has been undertaken previously [42, 50, 51], we model the concentration of ppGpp being proportional to the charged (tRNA*) to uncharged (tRNA) balance,

$$[\text{ppGpp}] \propto \frac{1}{\frac{\text{tRNA}^*}{\text{tRNA}}}. \tag{12}$$

The dynamics of the charged- and uncharged-tRNA pools themselves are determined by the activity of metabolic proteins and translation with the translation rate $\gamma = \gamma(tRNA^*)$ and the metabolic rate $\nu = \nu(tRNA)$ depending on the absolute availability of each tRNA pool, respectively. The structure of this extended model, which we term the *flux-parity allocation model*, is outlined diagrammatically in Fig. 3(D). It can produce nearly identical behavior to scenario III of the simple allocation model where we enforced optimal allocation by hand [Fig. 3(E) and (F)]. A more detailed mathematical definition of the flux-parity model and an analysis how growth varies with the model parameters to describe ppGpp dynamics is provided in Supplemental Text 11. Notably, optimal allocation does not require specific parameter values but holds for a large subset of combinations, supporting the idea that a flux-parity regulation ensuring an optimal allocation of ribosomes can evolve, provided that feedback systems tying gene regulation to the metabolic flux are in place.

The Flux-Parity Allocation Model Predicts Growth Behavior In and Out Of Steady-State

We find that the flux-parity allocation model is extremely versatile and allows us to quantitatively describe aspects of microbial growth in and out of steady-state and under various physiological stresses. We here demonstrate this versatility by comparing predictions to data for four particular examples using the same self-consistent set of parameters we have used thus far (Fig. 5).First, we examine the influence of translation-targeting antibiotics like chloramphenicol on steady-state growth in different growth media [39, 45] [Fig. 5(A, red shades)]. By incorporating a mathematical description of ribosome inactivation via binding to chloramphenicol, we find that the flux-parity allocation model quantitatively predicts the change in steady-state growth and ribosomal content with increasing chloramphenicol concentration (middle panel). Furthermore, the effect on the translation speed is qualitatively captured (right panel and Supplementary Text 11). The ability of the flux-parity allocation model to describe these effects without readjustment of the model is notable and provides a mechanistic rationale for the phenomenological relations previously established [39, 45].

Second, we consider the burden of excess protein synthesis by examining the expression of synthetic genes [Fig. 5(B)]. The middle panel shows the decrease of growth rates when cells are forced to synthesize different amounts of the lactose cleaving enzyme β-galactosidase in different media lacking lactose (red shades). The flux-parity allocation model (dashed lines) quantitatively predicts the change in growth rate with the measured fraction of β-galactosidase without further fitting (Supplementary Text 11). The trends for different media (red shades) quantitatively collapse onto a single line (right panel) when comparing changes in relative growth rates, a relation which is also captured by the model (dashed black line) and furthermore holds for other proteins (symbols). This collapse demonstrates that the flux-parity allocation model is able to describe excess protein synthesis in general, rather than at molecule- or media-specific level.

We also probed growth dynamics in fluctuating environments [Fig. 5(C and D)]. As a third example, we examine growth in an environment where the quality of the nutrients shifts from poor to rich by the sudden appearance of another carbon source. The middle panel shows three examples of such nutritional upshifts (markers), all of which are well described by the flux-parity allocation theory (dashed lines). The precise values of the growth rates before, during, and after the shift will depend on the specific carbon sources involved. However, by relating the growth rates before and immediately after the shift to the total shift magnitude (as shown in Ref. [55]), one can collapse a large collection of data onto a single curve (markers, right-panel). The collapse emerges naturally from the model

(dashed-line) when decomposing the metabolic sector into needed and non-needed components (Supplementary Text 11), demonstrating that the flux-parity allocation model is able to quantitatively describe nutritional upshifts at a fundamental level.

As a final example, we consider growth dynamics during the onset of starvation, another non steady-state phenomenon [Fig. 5(D)]. The middle panel shows the growth of batch cultures where glucose is provided as the sole carbon source in different limiting concentrations [76] (markers). The cessation of growth coincides with a rapid, ppGpp-mediated increase in expression of metabolic proteins [72, 77]. Bren et al. [76] demonstrated that expression from a glucose-specific metabolic promoter (PtsG) rapidly, yet temporarily, increases with the peak occurring at the moment where growth abruptly stops (right panel, solid lines). The flux-parity allocation model again predicts this behavior at a quantitative level without ad-hoc fitting (Supplementary Text 11), cementing the ability of the model to describe growth far from steady-state.

In summary, the model including flux-parity regulation of ribosomal allocation can capture a diverse array of phenomena using a singular reference parameter set. This includes phenomena in and out of steady-state, and even across engineered physiological stresses, demonstrating that this model encapsulates the underlying cellular circuitry and acts as a fundamental principle defining growth in nutrient-replete conditions.

Discussion

Microbial growth results from the orchestration of an astoundingly diverse set of biochemical reactions mediated by thousands of protein species. Despite this enormous complexity, experimental and theoretical studies alike have shown that many growth phenotypes can be captured by relatively simple correlations and models which incorporate only a handful of parameters [7, 39, 45, 48–52, 55]. Through re-examination of these works, we relax commonly invoked approximations and assumptions (Supplemental Text 1), include a generalized description of global regulation, and integrate an extensive comparison with data to establish a self-consistent, low-dimensional model of protein synthesis that is capable of quantitatively describing complex growth behaviors in and out of steady-state.

Growth emerges in this model as a consequence of protein synthesis and the allocation of ribosome activity towards (i) making new ribosomes, (ii) making the metabolic proteins which sustain the precursors ribosomes require to translate, and (iii) making other proteins cells require to operate. An *optimal allocation* which yields the fastest growth in a given condition is reached when the synthesis of precursors (metabolic flux) and the consumption of precursors (translational flux) are mutually maximized, a process we term *flux-parity regulation*. We analyze how such regulation can be mechanistically achieved by the relative sensing of charged- and uncharged-tRNA via the abundance of a global regulator (such as ppGpp) which diametrically affects the expression of ribosomal and metabolic genes. Through extensive comparison with 52 data sets from 37 studies, we show that the flux-parity model predicts the fundamental growth behavior of *E. coli* with quantitative accuracy. Beyond the impeccable description of the growth-rate dependent ribosomal content and translation speed across various carbon sources, the flux-parity model quantitatively captures phenomena out of steady-state (including nutrient upshifts and response to starvation) and under externally applied physiological perturbations (such as antibiotic stress or expression of synthetic genes). Notably, the broad agreement across data sets is obtained using a single core parameter set which does not require any adjustment from one scenario to the next. As such, the flux-parity model predicts the microbial "growth laws", providing a mechanistic explanation for previous phenomenological models formulated to understand them [45, 48, 49]. The finding that these predictions hold so well despite the overwhelmingly complex nature of the cell further demonstrates that biological systems are not irreducibly complex but can be distilled to a small number of principal components sufficient to capture the core behavior of the system.

As proteins commonly account for the majority of biomass in microbial organisms and the core processes of protein synthesis are universally conserved among them, it is likely that protein synthesis is a fundamental growth constraint across organisms. Accordingly, flux-parity regulation may be a very general scheme which ensures the efficient coordination of metabolic and translational fluxes across many microbial organisms. And as our modeling approach is organism-agnostic, it should be transferable to a variety of microbes growing in nutrient-replete conditions. Indeed, other organisms including *S. cerevisiae* (Supplementary Text 10) exhibit a strict interdependence between growth rate and ribosome content [18], as is predicted by the flux-parity model. However, more quantitative

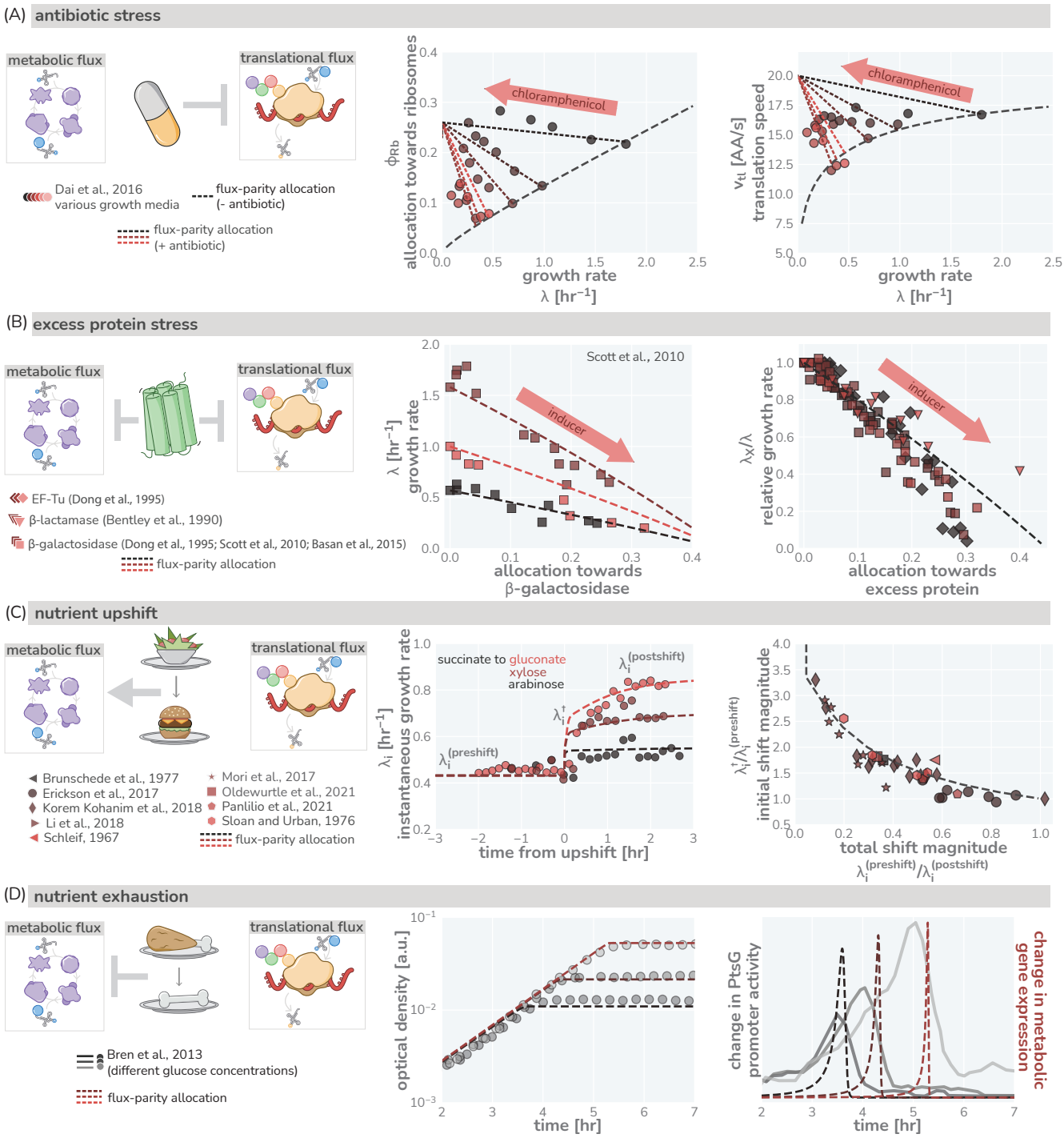

Figure 5: Flux-parity regulation describes optimal growth of *E. coli* under physiological perturbations and out of steady state. (A) Inhibition of ribosome activity via antibiotic modeled repression of translational flux. Plots show comparison with data for different media (red shades) with the flux-parity model predictions (dashed lines). (B) Inhibition of metabolic and translational fluxes through excess gene expression. Middle panel shows data where β-galactosidase is expressed at different levels. Different shades of red correspond to different growth media. Right-hand panel shows collapse of the growth rates of overexpression of β-galactosidase (squares), β-lactamase (inverted triangles), and EF-Tu (diamonds) relative to the wild-type growth rate in different media conditions. (C) Nutrient-upshifts increase the metabolic flux. Middle panel shows the instantaneous growth rate λ_i for shifts from succinate to gluconate (bright red), xylose (dark red), or arabinose (black) [52]. Right-hand panel shows collapse of instantaneous growth rate measurements immediately after the shift (relative to the preshift-growth rate) as a function of the total shift magnitude. (D) Exhaustion of nutrients in the environment yields a decrease in the metabolic flux, promoting expression of more metabolic proteins. Middle panel shows growth curve measurements in media with different starting concentrations of glucose (0.22 mM, 0.44 mM, and 1.1 mM glucose from light to dark, respectively) overlaid with flux-parity predictions. Right-hand panel shows the change in total metabolic protein synthesis in the flux-parity model (dashed lines) overlaid with the change in expression of a fluorescent reporter from a PtsG promoter (solid lines).

data on ribosomal content, translation speeds, upshift dynamics, and more need to be acquired to fully examine the commonality of flux-parity regulation in the microbial world.

A common interpretation of previous allocation models is that cells maximize their growth rate in encountered conditions, which implies that cells have some means to perceive their own growth rate [42, 47, 50]. We challenge this interpretation as flux-parity regulation only ensures optimal coordination between metabolic and translational fluxes and does not imply that growth rate is maximized nor directly sensed (Supplementary Text 11). In particular, the flux-parity model does not assume that the pool of metabolic proteins is tailored to maximize the metabolic flux and thus growth in the encountered conditions. This is in agreement with an expansive body of evidence that shows that microbes frequently synthesize metabolic and other proteins which are not directly needed in the encountered condition and thus impede growth. *E. coli*, for example, synthesizes a plethora of different transport proteins when exposed to poor growth conditions even if the corresponding substrates are not available, collectively occupying a significant portion of the proteome [27, 33, 46]. Accordingly, it has been observed that cells stop synthesizing these proteins when evolving in the absence of those sugars [78, 79].

But why, then, do we observe an optimal allocation between metabolic and ribosomal proteins when the pool of metabolic proteins itself shows this apparent non-optimal behavior? We posit here that both behaviors emerge from the adaptation to fluctuating conditions: In contrast to the well-defined static conditions of laboratory experiments, the continuous ebb and flow of nutrients in natural environments precludes any sense of stability. Accordingly, the machinery of the cell should be predominantly adapted to best cope with the fluctuating conditions microbial organisms encounter in their natural habitats. A complex regulation of metabolic proteins is thus expected, including for example, the diverse expression of nutrient transporters which promote growth in anticipated conditions, rather than synthesizing only those specific to nutrients that are present in the moment [80].

However, in those fluctuating conditions, flux-parity regulation is required to ensure rapid growth. To illustrate this point, we consider again a nutrient upshift in which there is an instantaneous improvement in the nutrient conditions. We compare the predicted response via flux-parity [Fig. 6 (B, red box)] with that predicted by a simpler step-wise regulation where the allocation solely depends on the environmental condition (and not the internal fluxes) and immediately adjusts to the new steady value at the moment of the shift [Fig. 6 (B, blue box)]. The dynamic reallocation by flux-parity facilitates a sharp increase in the allocation towards ribosomes [Fig. 6(C)], resulting in a rapid increase in instantaneous growth rate compared to the step-wise reallocation mechanism [Fig. 6(D)], suggesting that flux-parity is advantageous in fluctuating environments. As its regulation solely depends on the internal state of the cell (meaning, the relative abundance of charged- to uncharged-tRNA) it holds independently of the encountered conditions. This stands in contrast to the regulation of metabolic proteins, where both the external and internal states dictate what genes are expressed. As a result, optimal coordination between metabolic and translational fluxes occurs ubiquitously across conditions and not only in those that occur in natural habitats and drive adaptation. These broader conditions include steady-state growth within the laboratory, with the "growth laws" observed under those conditions emerging as a serendipitous consequence.

In summary, we view the process of cellular decision making as having two major components [Fig. 6(D)]: (i) determining what metabolic genes should be expressed given the environmental and physiological state and (ii) determining how ribosomes should be allocated given the metabolic and translational fluxes. Flux-parity regulation can explain the latter but many details of the former remain unknown. Additional studies are thus required to understand how the regulation of metabolic genes depends on encountered conditions and how it is shaped by adaptation to specific habitats. However, the ability of the presented modeling approach to predict complex phenotypes across scales suggests that it can also act as a basis to answer these questions, and thereby galvanize an integrative understanding of microbial life connecting physiology, ecology, and evolution.

Data and Code Availability

This work is accompanied by a website (`cremerlab.github.io/flux_parity`) which houses a suite of interactive figures to help the reader gain an intuition for the way the theory operates. Data sets can be downloaded individually from this website. Alternatively, all data and Python code used in this work can be cloned as a GitHub repository (`github.com/cremerlab/flux_parity`). This repository and its releases are also available via Zendodo with the DOI: 10.5281/zenodo.5893800.

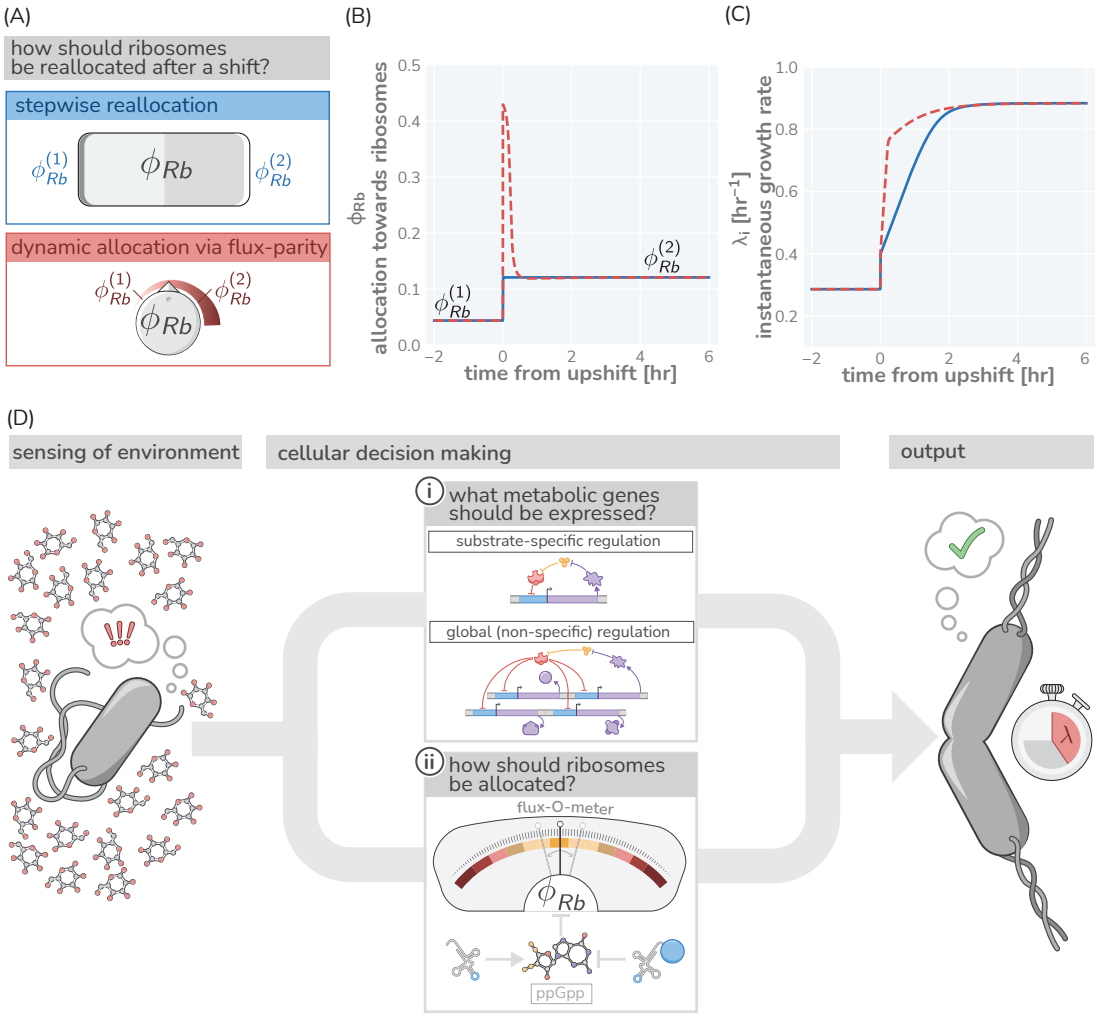

Figure 6: Flux parity allocation as a strategy to adapt to fluctuating conditions. (A) Ribosome reallocation strategies upon a nutrient upshift. After a nutrient upshift, cells either dynamically reallocate their ribosomes given flux-parity regulation (top, red) or they undergo stepwise reallocation from one steady-state value to the next (bottom, blue). (B) The allocation dynamics for both strategies in response to a nutrient upshift. (C) The instantaneous growth rate for both strategies over the course of the shift. Dashed red and solid blue lines correspond to model predictions for optimal allocation and flux-parity regulation, respectively. (D) Cellular decision making in fluctuating environments. Upon sensing features of the environment, cells undergo a two-component decision making protocol defining what metabolic genes should be expressed (top) and how the allocation towards ribosomes should be adjusted to maintain flux-parity. The combination of these processes yield an increase of biomass at a given characteristic growth rate.

Acknowledgments

We thank Uri Alon, Markus Arnoldini, Rachel Banks, Suzy Beeler, Nathan Belliveau, Soichi Hirokawa, Christine Jacobs-Wagner, Sergey Kryazhimskiy, Armita Nourmohammad, Manuel Razo-Mejia, Tom Röschinger, Jan Skotheim, Cat Triandafillou, and members of the groups of Dmitri Petrov, Alfred Spormann, and JC for extensive discussions and the critical reading of the manuscript. GC acknowledges support by the NSF Postdoctoral Research Fellowships in Biology Program (Grant No. 2010807).

References

[1] Jacques Monod. Le taux de croissance en fonction d la concntration de l'aliment dans une population de *Glaucoma piriformis* en culture pure. *Comtes Rendus des Séances de l'Académie des Sciences*, (201):1513–1515, 1935.

[2] Jacques Monod. Ratio d'entretien et ration de croissance dan les populations bactériennes. *Comtes Rendus des Séances de l'Académie des Sciences*, (205):1456–1457, 1937.

[3] Jacques Monod. Sur un phénomene nouveau de croissance complexe dans les cultures bactériennes. *Comptes Rendus des Séances de l'Académie des Sciences*, 212:934–939, 1941.

[4] Jacques Monod. The phenomenon of enzymatic adaptation and its bearings on problems of genetics and cellular differentiation. *Growth Symposium*, 9:223–289, 1947.

[5] Jacques Monod. From enzymatic adaptation to allosteric transitions. *Science*, 154(3748):475–483, October 1966.

[6] Allan Campbell. Synchronization of Cell Division. *Bacteriol Rev*, 21:10, 1957.

[7] M. Schaechter, O. Maaløe, and N. O. Kjeldgaard. Dependency on medium and temperature of cell size and chemical composition during balanced growth of *Salmonella typhimurium*. *Microbiology*, 19(3):592–606, 1958.

[8] N. O. Kjeldgaard, O. Maaløe, and M. Schaechter. The Transition Between Different Physiological States During Balanced Growth of *Salmonella typhimurium*. *Journal of General Microbiology*, 19(3):607–616, December 1958.

[9] Stephen Cooper and Charles E. Helmstetter. Chromosome replication and the division cycle of *Escherichia* coli Br. *Journal of Molecular Biology*, 31(3):519–540, February 1968.

[10] W. D. Donachie, K. J. Begg, and M. Vicente. Cell length, cell growth and cell division. *Nature*, 264(5584):328–333, November 1976.

[11] Suckjoon Jun, Fangwei Si, Rami Pugatch, and Matthew Scott. Fundamental principles in bacterial physiology - history, recent progress, and the future with focus on cell size control: A review. *Reports on Progress in Physics*, 81(5):056601, May 2018.

[12] M Heldal, S Norland, and O Tumyr. X-ray microanalytic method for measurement of dry matter and elemental content of individual bacteria. *Applied and Environmental Microbiology*, 50(5):1251–1257, November 1985.

[13] M. Loferer-Krößbacher, J. Klima, and R. Psenner. Determination of Bacterial Cell Dry Mass by Transmission Electron Microscopy and Densitometric Image Analysis. *Applied and Environmental Microbiology*, 64(2):688–694, February 1998.

[14] Hugh G Lawford and Joyce D Rousseau. Studies on Nutrient Requirements and Cost-Effective Supplements for Ethanol Production by Recombinant E. coli. *Applied Biochemistry and Biotechnology*, 57:20, 1996.

[15] T. G Watson. Amino-acid Pool Composition of *Saccharomyces cerevisiae* as a Function of Growth Rate and Amino-acid Nitrogen Source. *Journal of General Microbiology*, 96(2):263–268, 1976.

[16] R. J. Britten and Clure Ft Mc. The amino acid pool in *Escherichia coli*. *Bacteriol Rev*, 26:292–335, September 1962.

[17] Kirsten Gausing. Regulation of ribosome production in *escherichia* coli: Synthesis and stability of ribosomal RNA and of ribosomal protein messenger RNA at different growth rates. *Journal of Molecular Biology*, 115(3):335–354, September 1977.

[18] Tatiana V. Karpinets, Duncan J. Greenwood, Carl E. Sams, and John T. Ammons. RNA:protein ratio of the unicellular organism as a characteristic of phosphorous and nitrogen stoichiometry and of the cellular requirement of ribosomes for protein synthesis. *BMC Biology*, 4(1):30, September 2006.

[19] Arthur L. Koch. Why can't a cell grow infinitely fast? *Canadian Journal of Microbiology*, 34(4):421–426, April 1988. Publisher: NRC Research Press.

[20] V.J. Hernandez and H. Bremer. Characterization of RNA and DNA synthesis in *escherichia* coli strains devoid of ppGpp. *Journal of Biological Chemistry*, 268(15):10851–10862, May 1993.

[21] B. Magasanik, Adele K. Magasanik, and F. C. Neidhardt. Regulation of Growth and Composition of the Bacterial Cell. In *Ciba Foundation Symposium — Regulation of Cell Metabolism*, pages 334–352. John Wiley & Sons, Ltd, 1959. _eprint: https://onlinelibrary.wiley.com/doi/pdf/10.1002/9780470719145.ch16.

[22] Stephen M. Doris, Deborah R. Smith, Julia N. Beamesderfer, Benjamin J. Raphael, Judith A. Nathanson, and Susan A. Gerbi. Universal and domain-specific sequences in 23S–28S ribosomal RNA identified by computational phylogenetics. *RNA*, 21(10):1719–1730, October 2015.

[23] Chen Davidovich, Matthew Belousoff, Anat Bashan, and Ada Yonath. The evolving ribosome: From non-coded peptide bond formation to sophisticated translation machinery. *Research in Microbiology*, 160(7):487–492, September 2009.

[24] Christian M. Bruell, Carolin Eichholz, Andriy Kubarenko, Virginia Post, Vladimir I. Katunin, Sven N. Hobbie, Marina V. Rodnina, and Erik C. Böttger. Conservation of Bacterial Protein Synthesis Machinery: Initiation and Elongation in Mycobacterium smegmatis. *Biochemistry*, 47(34):8828–8839, August 2008.

[25] Y. Taniguchi, P. J. Choi, G. W. Li, H. Chen, M. Babu, J. Hearn, A. Emili, and X. S. Xie. Quantifying *E. coli* proteome and transcriptome with single-molecule sensitivity in single cells. *Science*, 329:533–8, July 2010.

[26] Bryson D. Bennett, Elizabeth H. Kimball, Melissa Gao, Robin Osterhout, Stephen J. Van Dien, and Joshua D. Rabinowitz. Absolute metabolite concentrations and implied enzyme active site occupancy in *Escherichia* coli. *Nature Chemical Biology*, 5(8):593–599, August 2009.

[27] Alexander Schmidt, Karl Kochanowski, Silke Vedelaar, Erik Ahrné, Benjamin Volkmer, Luciano Callipo, Kèvin Knoops, Manuel Bauer, Ruedi Aebersold, and Matthias Heinemann. The quantitative and condition-dependent *Escherichia coli* proteome. *Nature Biotechnology*, 34(1):104–110, January 2016.

[28] Kaspar Valgepea, Kaarel Adamberg, Andrus Seiman, and Raivo Vilu. *Escherichia coli* achieves faster growth by increasing catalytic and translation rates of proteins. *Molecular BioSystems*, 9(9):2344–2358, July 2013.

[29] Karl Peebo, Kaspar Valgepea, Andres Maser, Ranno Nahku, Kaarel Adamberg, and Raivo Vilu. Proteome reallocation in *Escherichia coli* with increasing specific growth rate. *Molecular BioSystems*, 11(4):1184–1193, 2015.

[30] Gene-Wei Li, David Burkhardt, Carol Gross, and Jonathan S. Weissman. Quantifying absolute protein synthesis rates reveals principles underlying allocation of cellular resources. *Cell*, 157(3):624–635, April 2014.

[31] Rohan Balakrishnan, Matteo Mori, Igor Segota, Zhongge Zhang, Ruedi Aebersold, Christina Ludwig, and Terence Hwa. Principles of gene regulation quantitatively connect DNA to RNA and proteins in bacteria. *bioRxiv*, page 2021.05.24.445329, May 2021.

[32] Matteo Mori, Zhongge Zhang, Amir Banaei-Esfahani, Jean-Benoît Lalanne, Hiroyuki Okano, Ben C Collins, Alexander Schmidt, Olga T Schubert, Deok-Sun Lee, Gene-Wei Li, Ruedi Aebersold, Terence Hwa, and Christina Ludwig. From coarse to fine: The absolute *Escherichia coli* proteome under diverse growth conditions. *Molecular Systems Biology*, 17(5), May 2021.

[33] Nathan M. Belliveau, Griffin Chure, Christina L. Hueschen, Hernan G. Garcia, Jane Kondev, Daniel S. Fisher, Julie A. Theriot, and Rob Phillips. Fundamental limits on the rate of bacterial growth and their influence on proteomic composition. *Cell Systems*, July 2021.

[34] Eyal Metzl-Raz, Moshe Kafri, Gilad Yaakov, Ilya Soifer, Yonat Gurvich, and Naama Barkai. Principles of cellular resource allocation revealed by condition-dependent proteome profiling. *eLife*, 6:e28034, August 2017.

[35] Joao A. Paulo, Jeremy D. O'Connell, Aleksandr Gaun, and Steven P. Gygi. Proteome-wide quantitative multiplexed profiling of protein expression: Carbon-source dependency in *Saccharomyces cerevisiae*. *Molecular Biology of the Cell*, 26(22):4063–4074, November 2015.

[36] Joao A. Paulo, Jeremy D. O'Connell, Robert A. Everley, Jonathon O'Brien, Micah A. Gygi, and Steven P. Gygi. Quantitative mass spectrometry-based multiplexing compares the abundance of 5000 S. *cerevisiae* proteins across 10 carbon sources. *Journal of Proteomics*, 148:85–93, October 2016.

[37] Jianye Xia, Benjamin Sánchez, Yu Chen, Kate Campbell, Sergo Kasvandik, and Jens Nielsen. Proteome allocations change linearly with specific growth rate of *Saccharomyces cerevisiae* under glucose-limitation. Preprint, In Review, May 2021.

[38] Michael Jahn, Vital Vialas, Jan Karlsen, Gianluca Maddalo, Fredrik Edfors, Björn Forsström, Mathias Uhlén, Lukas Käll, and Elton P. Hudson. Growth of Cyanobacteria Is Constrained by the Abundance of Light and Carbon Assimilation Proteins. *Cell Reports*, 25(2):478–486.e8, October 2018.

[39] Xiongfeng Dai, Manlu Zhu, Mya Warren, Rohan Balakrishnan, Vadim Patsalo, Hiroyuki Okano, James R. Williamson, Kurt Fredrick, Yi-Ping Wang, and Terence Hwa. Reduction of translating ribosomes enables *Escherichia* coli to maintain elongation rates during slow growth. *Nature Microbiology*, 2(2):1–9, December 2016.

[40] Markus Basan, Manlu Zhu, Xiongfeng Dai, Mya Warren, Daniel Sévin, Yi-Ping Wang, and Terence Hwa. Inflating bacterial cells by increased protein synthesis. *Molecular Systems Biology*, 11(10):836, October 2015.

[41] Conghui You, Hiroyuki Okano, Sheng Hui, Zhongge Zhang, Minsu Kim, Carl W. Gunderson, Yi-Ping Wang, Peter Lenz, Dalai Yan, and Terence Hwa. Coordination of bacterial proteome with metabolism by cyclic AMP signalling. *Nature*, 500(7462), August 2013.

[42] Chenhao Wu, Rohan Balakrishnan, Matteo Mori, Gabriel Manzanarez, Zhongge Zhang, and Terence Hwa. Cellular perception of growth rate and the mechanistic origin of bacterial growth laws. Preprint, Systems Biology, October 2021.

[43] Francesca Di Bartolomeo, Carl Malina, Kate Campbell, Maurizio Mormino, Johannes Fuchs, Egor Vorontsov, Claes M. Gustafsson, and Jens Nielsen. Absolute yeast mitochondrial proteome quantification reveals trade-off between biosynthesis and energy generation during diauxic shift. *Proceedings of the National Academy of Sciences*, 117(13):7524–7535, March 2020. Publisher: National Academy of Sciences Section: Biological Sciences.

[44] Sophia Hsin-Jung Li, Zhiyuan Li, Junyoung O. Park, Christopher G. King, Joshua D. Rabinowitz, Ned S. Wingreen, and Zemer Gitai. *Escherichia coli* translation strategies differ across carbon, nitrogen and phosphorus limitation conditions. *Nature Microbiology*, 3(8), August 2018.

[45] Matthew Scott, Carl W. Gunderson, Eduard M. Mateescu, Zhongge Zhang, and Terence Hwa. Interdependence of Cell Growth and Gene Expression: Origins and Consequences. *Science*, 330(6007):1099–1102, November 2010.

[46] Sheng Hui, Josh M. Silverman, Stephen S. Chen, David W. Erickson, Markus Basan, Jilong Wang, Terence Hwa, and James R. Williamson. Quantitative proteomic analysis reveals a simple strategy of global resource allocation in bacteria. *Molecular Systems Biology*, 11(2), February 2015.

[47] Benjamin D. Towbin, Yael Korem, Anat Bren, Shany Doron, Rotem Sorek, and Uri Alon. Optimality and sub-optimality in a bacterial growth law. *Nature Communications*, 8(1):14123, April 2017.

[48] Douwe Molenaar, Rogier van Berlo, Dick de Ridder, and Bas Teusink. Shifts in growth strategies reflect tradeoffs in cellular economics. *Molecular Systems Biology*, 5(1):323, January 2009.

[49] M. Scott, S. Klumpp, E. M. Mateescu, and T. Hwa. Emergence of robust growth laws from optimal regulation of ribosome synthesis. *Molecular Systems Biology*, 10(8):747–747, August 2014.

[50] Evert Bosdriesz, Douwe Molenaar, Bas Teusink, and Frank J. Bruggeman. How fast-growing bacteria robustly tune their ribosome concentration to approximate growth-rate maximization. *The FEBS journal*, 282(10):2029–2044, May 2015.

[51] Nils Giordano, Francis Mairet, Jean-Luc Gouzé, Johannes Geiselmann, and Hidde de Jong. Dynamical Allocation of Cellular Resources as an Optimal Control Problem: Novel Insights into Microbial Growth Strategies. *PLOS Computational Biology*, 12(3):e1004802, March 2016.

[52] David W. Erickson, Severin J. Schink, Vadim Patsalo, James R. Williamson, Ulrich Gerland, and Terence Hwa. A global resource allocation strategy governs growth transition kinetics of *Escherichia coli*. *Nature*, 551(7678):119–123, November 2017.

[53] Francis Mairet, Jean-Luc Gouzé, and Hidde de Jong. Optimal proteome allocation and the temperature dependence of microbial growth laws. *npj Systems Biology and Applications*, 7(1):1–11, March 2021.

[54] Diana Serbanescu, Nikola Ojkic, and Shiladitya Banerjee. Nutrient-Dependent Trade-Offs between Ribosomes and Division Protein Synthesis Control Bacterial Cell Size and Growth. *Cell Reports*, 32(12), September 2020.

[55] Yael Korem Kohanim, Dikla Levi, Ghil Jona, Benjamin D. Towbin, Anat Bren, and Uri Alon. A Bacterial Growth Law out of Steady State. *Cell Reports*, 23(10):2891–2900, June 2018.

[56] Gordon Churchward, Hans Bremer, and Ry Young. Macromolecular composition of bacteria. *Journal of Theoretical Biology*, 94(3):651–670, February 1982.

[57] Francisco Feijó Delgado, Nathan Cermak, Vivian C. Hecht, Sungmin Son, Yingzhong Li, Scott M. Knudsen, Selim Olcum, John M. Higgins, Jianzhu Chen, William H. Grover, and Scott R. Manalis. Intracellular Water Exchange for Measuring the Dry Mass, Water Mass and Changes in Chemical Composition of Living Cells. *PLOS ONE*, 8(7):e67590, July 2013. Publisher: Public Library of Science.

[58] A. H. Stouthamer. A theoretical study on the amount of ATP required for synthesis of microbial cell material. *Antonie van Leeuwenhoek*, 39(1):545–565, December 1973.

[59] Derek N. Macklin, Travis A. Ahn-Horst, Heejo Choi, Nicholas A. Ruggero, Javier Carrera, John C. Mason, Gwanggyu Sun, Eran Agmon, Mialy M. DeFelice, Inbal Maayan, Keara Lane, Ryan K. Spangler, Taryn E. Gillies, Morgan L. Paull, Sajia Akhter, Samuel R. Bray, Daniel S. Weaver, Ingrid M. Keseler, Peter D. Karp, Jerry H. Morrison, and Markus W. Covert. Simultaneous cross-evaluation of heterogeneous *e. coli* datasets via mechanistic simulation. *Science*, 369(6502), July 2020.

[60] Jonathan R. Karr, Jayodita C. Sanghvi, Derek N. Macklin, Miriam V. Gutschow, Jared M. Jacobs, Benjamin Bolival, Nacyra Assad-Garcia, John I. Glass, and Markus W. Covert. A Whole-Cell Computational Model Predicts Phenotype from Genotype. *Cell*, 150(2):389–401, July 2012.

[61] Pranas Grigaitis, Brett G. Olivier, Tomas Fiedler, Bas Teusink, Ursula Kummer, and Nadine Veith. Protein cost allocation explains metabolic strategies in *Escherichia* coli. *Journal of Biotechnology*, 327:54–63, February 2021.

[62] Chalongrat Noree, Kyle Begovich, Dane Samilo, Risa Broyer, Elena Monfort, and James E. Wilhelm. A quantitative screen for metabolic enzyme structures reveals patterns of assembly across the yeast metabolic network. *Molecular Biology of the Cell*, 30(21):2721–2736, October 2019.

[63] Jes Forchhammer and Lasse Lindahl. Growth rate of polypeptide chains as a function of the cell growth rate in a mutant of *Escherichia* coli. *Journal of Molecular Biology*, 55(3):563–568, February 1971.

[64] Måns Ehrenberg and C. G. Kurland. Costs of accuracy determined by a maximal growth rate constraint. *Quarterly Reviews of Biophysics*, 17(1):45–82, February 1984. Publisher: Cambridge University Press.

[65] Stefan Klumpp, Matthew Scott, Steen Pedersen, and Terence Hwa. Molecular crowding limits translation and cell growth. *Proceedings of the National Academy of Sciences*, 110(42):6, 2013.

[66] Jacques Monod. The Growth of Bacterial Cultures. *Annual Review of Microbiology*, 3:371–394, 1949.

[67] E Martínez-Salas, J A Martín, and M Vicente. Relationship of *escherichia coli* density to growth rate and cell age. *Journal of Bacteriology*, 147(1):97–100, July 1981.

[68] H E Kubitschek, W W Baldwin, and R Graetzer. Buoyant density constancy during the cell cycle of *escherichia* coli. *Journal of Bacteriology*, 155(3):1027–1032, September 1983. Publisher: American Society for Microbiology.

[69] Patrick P. Dennis and Hans Bremer. Differential rate of ribosomal protein synthesis in *escherichia* coli B/r. *Journal of Molecular Biology*, 84(3):407–422, April 1974.

[70] Ludovico Calabrese, Jacopo Grilli, Matteo Osella, Christopher P. Kempes, Marco Cosentino Lagomarsino, and Luca Ciandrini. Role of protein degradation in growth laws. Technical report, August 2021. Company: Cold Spring Harbor Laboratory Distributor: Cold Spring Harbor Laboratory Label: Cold Spring Harbor Laboratory Section: New Results Type: article.

[71] Albert L. Müller, Wenyu Gu, Vadim Patsalo, Jörg S. Deutzmann, James R. Williamson, and Alfred M. Spormann. An alternative resource allocation strategy in the chemolithoautotrophic archaeon *Methanococcus maripaludis*. *Proceedings of the National Academy of Sciences*, 118(16), April 2021.

[72] Lisa U. Magnusson, Anne Farewell, and Thomas Nyström. ppGpp: a global regulator in *Escherichia coli*. *Trends in Microbiology*, 13(5):236–242, May 2005.

[73] Brent W. Anderson, Danny K. Fung, and Jue D. Wang. Regulatory Themes and Variations by the Stress-Signaling Nucleotide Alarmones (p)ppGpp in Bacteria. *Annual Review of Genetics*, 55(1), 2021. _eprint: https://doi.org/10.1146/annurev-genet-021821-025827.

[74] Katarzyna Potrykus, Helen Murphy, Nadège Philippe, and Michael Cashel. ppGpp is the major source of growth rate control in E. coli. *Environmental microbiology*, 13(3):563–575, March 2011.

[75] Katarzyna Potrykus and Michael Cashel. (p)ppGpp: Still Magical? *Annual Review of Microbiology*, 62(1):35–51, 2008. _eprint: https://doi.org/10.1146/annurev.micro.62.081307.162903.

[76] Anat Bren, Yuval Hart, Erez Dekel, Daniel Koster, and Uri Alon. The last generation of bacterial growth in limiting nutrient. *BMC Systems Biology*, 7(1):27, March 2013.

[77] Patrick P. Dennis, Mans Ehrenberg, and Hans Bremer. Control of rRNA Synthesis in *escherichia* coli: a Systems Biology Approach. *Microbiology and Molecular Biology Reviews*, 68(4):639–668, December 2004.

[78] Nicholas Leiby and Christopher J. Marx. Metabolic Erosion Primarily Through Mutation Accumulation, and Not Tradeoffs, Drives Limited Evolution of Substrate Specificity in *Escherichia coli*. *PLOS Biology*, 12(2):e1001789, February 2014.

[79] John S. Favate, Shun Liang, Srujana S. Yadavalli, and Premal Shah. The landscape of transcriptional and translational changes over 22 years of bacterial adaptation. *bioRxiv*, page 2021.01.12.426406, January 2021. Publisher: Cold Spring Harbor Laboratory Section: New Results.

[80] Rohan Balakrishnan, Roshali T de Silva, Terence Hwa, and Jonas Cremer. Suboptimal resource allocation in changing environments constrains response and growth in bacteria. *Molecular Systems Biology*, 17(12):e10597, December 2021. Publisher: John Wiley & Sons, Ltd.